

## Variable-temperature independently driven four-tip scanning tunneling microscope

Rei Hobara,<sup>a)</sup> Naoka Nagamura, and Shuji Hasegawa<sup>b)</sup>

*Department of Physics, School of Science, University of Tokyo, 7-3-1 Hongo, bunkyo-ku, Tokyo 113-0033, Japan*

Iwao Matsuda

*Synchrotron Radiation Laboratory, Institute for Solid State Physics, University of Tokyo, 5-1-5 Kashiwa-no-ha, Kashiwa, Chiba 277-8581, Japan*

Yuko Yamamoto, Yutaka Miyatake, and Toshihiko Nagamura

*UNISOKU Co., Ltd., 2-4-3, Kasugano, Hirakata, Osaka 573-0131, Japan*

(Received 18 January 2007; accepted 1 April 2007; published online 8 May 2007)

The authors have developed an ultrahigh vacuum (UHV) variable-temperature four-tip scanning tunneling microscope (STM), operating from room temperature down to 7 K, combined with a scanning electron microscope (SEM). Four STM tips are mechanically and electrically independent and capable of positioning in arbitrary configurations in nanometer precision. An integrated controller system for both of the multitip STM and SEM with a single computer has also been developed, which enables the four tips to operate either for STM imaging independently and for four-point probe (4PP) conductivity measurements cooperatively. Atomic-resolution STM images of graphite were obtained simultaneously by the four tips. Conductivity measurements by 4PP method were also performed at various temperatures with the four tips in square arrangement with direct contact to the sample surface. © 2007 American Institute of Physics. [DOI: 10.1063/1.2735593]

### I. INTRODUCTION

Conductivity measurements in submicron or nanometer scale are of great interest in nanoscience and nanotechnology. Several kinds of methods have been developed using, e.g., eddy current,<sup>1</sup> microwave,<sup>2</sup> and microscopic four-point probes.<sup>3-5</sup> In particular, a method which adopts tips of scanning tunneling microscope (STM) as electric probes has great advantages in positioning of probes in arbitrary configurations as well as in high spatial resolution of measurements.<sup>6-13</sup> By combining single-tip STM and patterned electrodes on the sample, Bachtold *et al.* measured electric properties of one-dimensional (1D) wires.<sup>6</sup> Kubo *et al.* developed a double-tip STM and measured metal nanowires by a two-point probe method in sub-100-nm probe spacing.<sup>11</sup> Shiraki and co-workers measured the conductivity of the surface state of Si crystals by four-point probe (4PP) method using a four-tip STM at various probe spacings.<sup>12,14</sup> It was also demonstrated that, owing to an advantage of the four-tip STM in which the four tips are positioned in arbitrary arrangements at aimed areas on the sample surface, a square arrangement of the four tips in 4PP method is useful to measure anisotropic conductivity<sup>15,16</sup>

Although, however, conductivity measurements using STM tips as electrodes are now popular, they are not yet done with temperature variation. This is because of a difficulty in integrating multitip STM with cooling system and scanning electron microscope (SEM) that is indispensable to

navigate the multitips. The system has to satisfy contradictory requirements for antimechanical vibration and thermal conduction. The cooling system requires firm connection between the sample and the cryostat for thermal conduction, and SEM also needs rigid fixation of the sample to the electron gun that is usually mounted on the outer chamber of the system. These rigid connections permit mechanical vibration to propagate from outside into the sample stage. On the other hand, STM usually needs mechanical isolation from the outside, because of its intolerance to the vibration. Usual single-tip STM can be constructed with a highly rigid actuator unit (tips, actuators, and sample) and/or with antivibration system. Since, however, the multitip STM inevitably have complex, asymmetric, and therefore less rigid actuator units because of the restriction of the space around sample, it needs mechanical isolation from the noisy surrounding, which is, on the contrary, against the cooling and SEM.

In this article, we report the development of a new four-tip STM operating at atomic resolution in simultaneous multitip scanning, at temperatures from room temperature (RT) down to 7 K in UHV, combined with SEM for tip positioning. In contrast to usual cryogenic STM, our STM stage is mounted above the cryostat thermally connected with a thick Cu rod, which ensures good thermal conduction and allows the SEM column placing above the stage. To overcome the vibration problem mentioned above, the STM stage can be switched between mechanically/thermally isolated from the chamber for STM operation and fixed for SEM/thermal conduction.

We have also developed an integrated controller for the multitip STM, which controls four STM tips as well as SEM

<sup>a)</sup>Electronic mail: rei@surface.phys.s.u-tokyo.ac.jp

<sup>b)</sup>URL: <http://surface.phys.s.u-tokyo.ac.jp/>

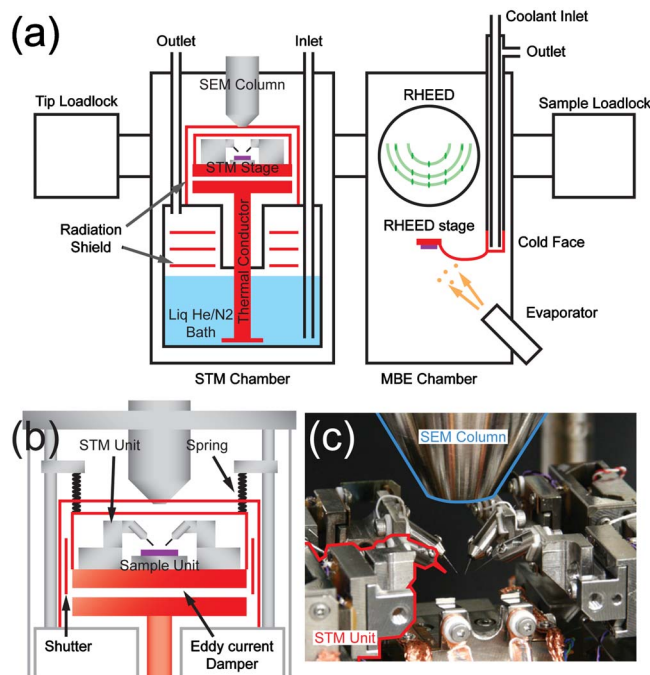


FIG. 1. (Color online) Schematic drawings of (a) the whole system and (b) around the STM stage. (c) A close-up photo of the STM stage without radiation shields. Red line surrounds one of the STM units. Blue line surrounds the SEM column.

simultaneously with a single personal computer (PC). It allows the four tips to operate either for STM imaging independently and for 4PP conductivity measurements cooperatively; each tip can be switched to be a current source/sink or a voltage probe. We demonstrate here the atomic-resolution STM imaging and variable-temperature conductivity measurements of a periodic array of In atomic wires on Si(111) surface.

## II. INSTRUMENTAL DESCRIPTION

Figures 1(a) and 1(b) show schematic drawings of the system, consisting of a main (STM) chamber, a sample preparation [molecular beam epitaxy (MBE)] chamber, and two load-lock chambers for sample and tip exchange. All chambers are UHV compatible and can keep the pressure down to  $10^{-9}$  Pa. The STM tips are installed into the main chamber from the tip load-lock chamber where a hot W filament is installed for outgassing of the tips. The sample is introduced from the MBE chamber where cleaning of the sample, deposition of materials, and reflection-high-energy electron diffraction (RHEED) observation can be done. The sample can be heated by direct current heating and cooled down to about 30 K by continuous flow cryostat in the MBE chamber. These capabilities are necessary for preparing aimed surface superstructures, epitaxial thin films, nanodots, nanowires, and so on.

The STM stage is mounted on the thermal conducting Cu rod, which is soaked in the coolant of the bath cryostat below. The STM stage including the sample and four actuator units is wholly surrounded with twofold radiation shields and movable shutters. This layout ensures efficient cooling and easy maintenance together with top placement of SEM

column. The photo of Fig. 1(c) is without the radiation shields. The sample can be cooled down to 7 K and be kept for 23 h with liquid He as coolant (0.6 l/h consumption). In the case of liquid N<sub>2</sub>, the minimum temperature is 80 K and the preserved time is longer than 3 days. STM stage and surrounding inner shield are cooled down to 6 K by the Cu rod directly. The outer shield is cooled to 100–150 K by the He exhaust gas. A secondary electron detector (SED) for SEM imaging is placed at the side of the outer shield.

The SEM column (APCO Mini-EOC) is mounted above the STM stage. The working distance of SEM is about 25 mm. The column touches softly with the outer shield. Although this thermally small connection cooled the bottom of column to about 200 K, we confirmed this cooling did not make thermal drift or degradation of resolution of SEM image. The electron beam is irradiated from SEM column through a 1 mm diameter hole in the outer shields. The maximum range of SEM field of view, which is about 2 mm, is not restricted by this hole but SEM electronics. The SEM image is obtained from the SED signal or beam induced current signal. The resolution of the SEM is about 20 nm for both of the signals.

A spring vibration isolator and an eddy current damper are built between the thermal conductor and the STM stage to avoid vibration of STM stage. The spring isolator decoupled the STM stage from other components at 2 Hz of resonant frequency. A Cu plate embedding more than 100 small samarium cobalt magnets is connected at the top of the thermal conducting rod. During SEM observation, tip/sample exchange, and cooling the stage, the STM stage is fixed to the thermal conductor and therefore the isolator and damper are disabled. When we fix the STM stage, the Cu plate functions as a thermal conductor and enlarges the contact area for good thermal connection. When we float the STM stage, this plate makes eddy current damper between the STM stage. Since alternative arrangements of the small magnets make closed magnetic paths, the magnetization does not affect SEM beam.

Four-tip actuator units are mounted at the corner of the square STM stage, and a sample actuator unit is placed at the center of the stage. The actuator units consist of stacked piezoceramics supported by sapphire plates. Each tip actuator unit controls three-dimensional motion by applying voltages to the stacked piezoceramics in two different ways as described below, while the sample actuator controls the XY directions only. For fine positioning or scanning in nanometer or subnanometer range, tips and sample are driven by ordinary piezoelectric effect. The maximum positioning range by this way is about  $2\ \mu\text{m}$  to each direction. For coarse positioning, the actuators can be driven by stick-slip mechanism in 5 mm travel distance in the XY directions and 2.5 mm in the Z direction at accuracy of 100 nm. In addition to these three- or two-dimensional-motion actuators, the tip actuators also contain small piezoceramics near the tips for fast STM feedback. Since the tips are sustained by actuator in cantilever style, the minimum resonant frequencies of tips are small relative to conventional straight style. Rough calculation shows that resonant frequency of cantilever style tips is about 800 Hz.

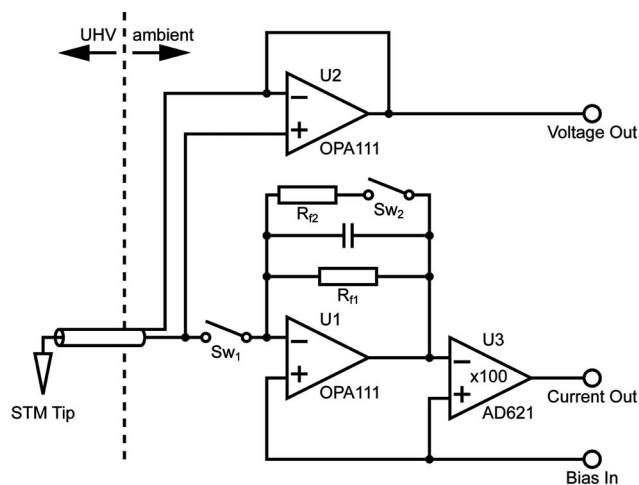


FIG. 2. A brief diagram of the preamp for one tip. A low-leakage operational amplifier (op-amp) (OPA111) U1 is used for the case of current probe to measure the tip current and to apply the bias voltage to the tip. Another op-amp U2 is installed in parallel to the signal line for the case of voltage probe to measure the tip voltage and to drive a guard of the signal line. Ultralow-leakage photo-MOS switches (MAX326) Sw<sub>1</sub> and Sw<sub>2</sub> are inserted in the signal line. The tip can be electrically insulated and work as a voltage probe by opening Sw<sub>1</sub>. When Sw<sub>1</sub> is closed, U1 and U3 measure the tip current, and the tip works as a current probe. Sw<sub>2</sub> switches the low- and high-current modes in the current-probe mode. R<sub>f1</sub> is 1–10 GΩ for low-current detection, while R<sub>f2</sub> is 1–10 MΩ for high-current detection.

We used a special technique for preparing W tips. The W tip made from a wire or rod by conventional DC electrochemical etching has a concave shape and has a big edge at the etching boundary. Since such an edge is an obstacle to approach several tips without touching each other, long conic-shape tips are suitable for the multitip STM. To make such a long conic tip, the tip was lifted up gradually from the solution during the etching. Tips made by this method are long, conic, and sharp with no edges of etching boundary.<sup>17</sup> Such a long conic W tip is also useful as a supporting tip for a carbon nanotube STM tip.<sup>18–20</sup>

Since, for 4PP conductivity measurements, the four STM tips should be not only independent but also cooperative, we have developed a special STM controller to control four tips in integrated ways. Four independent sets of STM electronics, conductivity measurement electronics, and SEM controller are integrated in this controller. It consists of four sets of switchable STM preamps and STM feedback circuits, SEM interface, analog-digital/digital-analog (AD/DA) interface, and a dedicated PC.

Figure 2 shows a simplified diagram of the preamp circuit for one tip. The preamp has some expansions special to the multitip STM; it enables the tip to be used as a low-current probe (<10 nA), a high-current probe (<10 μA), and a voltage probe by switching with internal semiconductor switches. In the current-probe mode, a bias voltage is applied to the tip and the tip current is monitored. The low-current mode is used for detecting tunneling contact and STM scanning, whereas both of low- and high-current modes are used for 4PP conductivity measurements depending on the resistance of the sample. In the voltage-probe mode, the tip is electrically floated and its electric potential (voltage) is monitored. This switching function is indispensable for the

multipurpose measurements by the four-tip STM. In 4PP conductivity measurements, two of the four tips are used as current source and sink probes while other two tips are used as voltage probes. The voltage-probe mode can be also used to apply electric field locally by the tip as a gate electrode. The same circuits are connected to the sample for adding more versatility to measurements.

All circuits of preamps were obliged to set outside the vacuum chamber because the electronics components are not UHV compatible, which is a disadvantage for low-current detection. Low capacitance cables with guard drive circuits and compensation circuits improve the sensitivity and bandwidth.<sup>22,23</sup> We confirmed that the total integral noise of the preamplifier was less than 1 pA at 1 kHz, which was enough performance for the STM and conductivity measurements.

By switching the mode of each preamp correctly, we can perform a variety of measurements. For STM operation, the tips work in low-current probe mode with different tip bias voltages. We can perform coarse/fine positioning, approaching of four tips, and STM/STS operation independently and simultaneously. For 4PP conductivity measurements, cooperation among the four tips is required. Starting with the condition that all tips are in tunneling contact to the sample surface, the integrated controller operates the following procedure quickly. (i) Arrange the four tips in an aimed arrangement with aid of SEM, with keeping tunneling contact for all tips. (ii) Stop the feedback circuit and fix the tip height. (iii) Change the bias voltage of all tips to zero or a low voltage to avoid short circuit. (iv) Extend the Z piezoactuators by a preset amount, and make direct contacts between tips and sample. The resistance between each tip and sample is set to be, e.g., less than 100 MΩ. (v) Switch two tips to the voltage-probe mode and the other two tips to (high or low) current-probe mode. (vi) Switch the sample preamp to the voltage-probe mode to avoid current leakage. (vii) Sweep the bias voltage between the current-probe tips, recording the current flowing through them and the voltage drop between the voltage-probe tips. (viii) Switch the preamps of all tips and sample to current-probe mode with zero or a low bias voltage. (ix) Shrink the Z piezoactuators and release the four tips. (x) Apply desired bias voltages to the tips to keep tunneling contact. (xi) Restart the feedback circuit. This sequence takes 1 ms–60 s depending on the sweep speed of bias voltage in step (vii). Because the piezoextension for making direct contact is small, the contact does not destroy the sample so much. No scars were observed by SEM after several repetition of this soft contact.

The controller has some useful functions. Since sample and tips are electrically connected to each current detector, the sample current and tip currents induced by the electron beam of SEM is detected separately. These signals are used to make images using the integrated controller as well as with usual SED signal. From images of tip currents, we obtain accurate position and shape of each tips. Tunneling contact for the four tips can be kept automatically by using both coarse and fine actuators for the Z direction. This is because the temperature drift of STM units is relatively large due to the asymmetric structure of the units. This function is useful

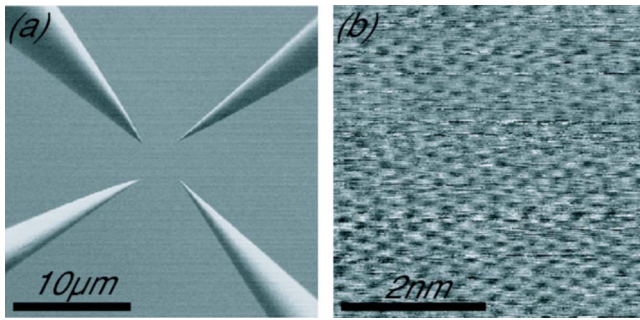


FIG. 3. (Color online) (a) SEM Image (with the SED signal) of the edgeless four W tips arranged in square of about  $5 \mu\text{m}$  side. (b) STM image of HOPG taken with one of the four tips. The tip bias is 0.2 V with tip current of 1.0 nA.

when the temperature is changed in wide range during 4PP conductivity measurements. The controller can execute measurement macros, which describe a sequence of measurement procedure such as approach of tips, arrangements of four tips, changing probe modes, and STM scanning.

### III. PERFORMANCE

We demonstrate here the basic performance of the present four-tip STM: STM/SEM observations and conductivity measurements by 4PP method in square tip arrangement at various temperatures.

#### A. SEM and STM

We can position the tips in about 200 nm accuracy by using stick-slip motion of actuators and 20 nm accuracy by using dc piezoelectric effect of actuators under SEM; the positioning accuracy is limited by the resolution of SEM. Figure 3(a) is a SEM image of the four tips arranged in square of about  $5 \mu\text{m}$  side. The tips have no edges of etching as mentioned in the previous section.<sup>17</sup>

The closest probe spacing is limited by interference between the tips and the accuracy of the contact position, which depends on the radius of tip apex. Since our W tips have typically about 50 nm radius of curvature at the ends, we cannot bring two tips any closer than about 100 nm. Carbon nanotube tips enable us to reduce the minimum probe spacing down to ca. 20 nm.<sup>19–21</sup>

Figure 3(b) is a STM image of highly oriented pyrolytic graphite (HOPG) for testing the STM capability. The honeycomb atomic structure of graphite can be seen although the noise in tunneling current is not small. The noise shows a peak at around 800 Hz, which is in good agreement with rough calculation of the lowest resonant frequency of our cantilever tip. We think that the end of cantilever tips are vibrated up and down easily and it causes the noise in the STM image.

The lowest resonant frequency limits the maximum frequency of the scan signal. Sawtooth voltage used in typical STM scanning contains high frequency harmonics which shake our less rigid tips irregularly during lateral scanning. Therefore 1–100 Hz sinusoidal voltage was used for the

scanning to reduce mechanical vibration of tips. Sinusoidal-voltage scanning is a gentle and fast way for less rigid scanners.

By measuring the tunneling current of a tip while other tips were scanning, it was confirmed that coupling of vibration between STM units was small enough compared with the vibration of STM unit caused by its own scanning. We also confirmed that STM imaging could be performed simultaneously without interference of STM scanning of other tips.

#### B. Conductivity measurements

We demonstrate here the capability of our four-tip STM by measuring anisotropic surface conductivity of a periodic array of In atomic chains on Si(111), Si(111)  $4 \times 1$ -In surface superstructure, by square-4PP method at various temperatures. The surface is known to have a quasi-one-dimensional metallic Fermi surface in the surface electronic state and therefore have highly anisotropic surface conductivity.<sup>15</sup> The square-4PP measurement where the four tips are arranged in square can provide the conductivity along the atomic chains and across them separately, while the linear 4PP measurement where the four tips are arranged on a line gives only a geometric average of the conductivities in both directions. This surface superstructure is also known to show a series of phase transition by cooling below RT ( $4 \times 1 \rightarrow 4 \times 2 \rightarrow 8 \times 2$ ) (Ref. 24) which cause a drastic decrease in surface conductivity.<sup>25</sup> Since, however, this was measured by the linear 4PP method with temperature variation, we did not yet know the temperature dependence of conductivities along the In chains and across them separately. It needs variable-temperature square-4PP measurements, which is now possible with our four-tip STM.

The standard procedure was used to prepare the  $4 \times 1$ -In surface in the MBE chamber.<sup>24</sup> A Si(111) [*n* type, 1–10  $\Omega \text{ cm}$  resistivity at RT,  $1.8^\circ$  off from the (111) plane] single-crystal wafer was flashed using direct current heating. Indium of 1.05 ML (ML denotes monolayer) was deposited at sample temperature of 450  $^\circ\text{C}$ . The ( $4 \times 1$ ) single-domain surface was confirmed at RT by RHEED. It was also confirmed that the surface structure changed from  $4 \times 1$  to  $4 \times 2$  around 150 K and from  $4 \times 2$  to  $8 \times 2$  around 90 K. Then, the sample was transferred to the STM chamber and cooled down to desired temperatures. The four tips were arranged in square of  $100 \mu\text{m}$  side, and made approach to the surface until the resistance between each tip and sample became smaller than 100 M $\Omega$ . We measured the current-voltage (*I*-*V*) curves in 4PP configuration by applying bias voltage (10–1000 mV) between the two current probes and measuring the voltage drop between two voltage probes.

Figure 4 is the measurement schematics (right bottom) and the results of *I*-*V* curves where the voltage difference between two voltage probes (tips *i* and *j*) ( $V_{ij}$ ) is measured while the current flowing between two current probes (tips *k* and *l*) ( $I_{kl}$ ) is swept by changing the bias voltage of the current probe. The In chains run vertically in this figure. The resistance parallel to the In chains ( $R_{\parallel}$ ) was derived from the slope of *I*-*V* curves  $R_{\parallel} = dV_{14}/dI_{23}$ . The resistance perpen-

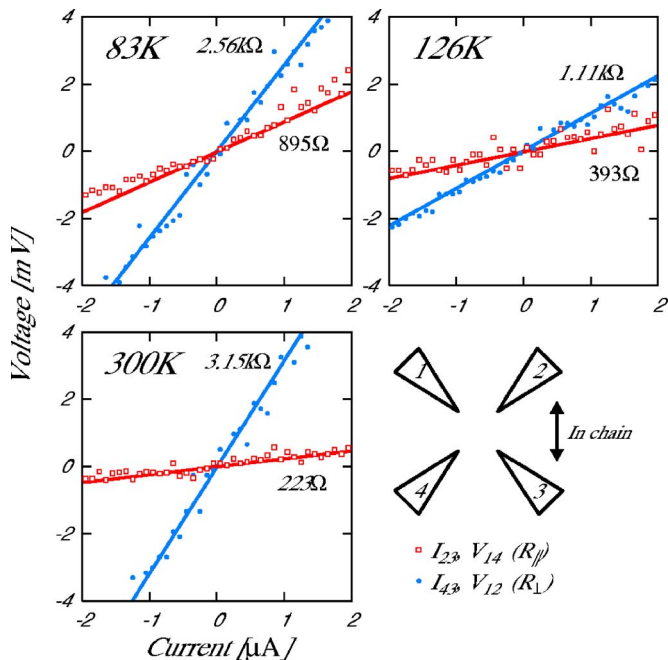


FIG. 4. (Color online) The current-voltage curves taken from Si(111)  $4 \times 1$ -In surface, by the square-4PP method at various temperatures. Filled circles are for  $R_{\perp} = dV_{12}/dI_{43}$ , and open squares are for  $R_{\parallel} = dV_{14}/dI_{23}$ , respectively. The In chains are aligned along the direction from tip 1(2) to tip 4(3).

pendicular to the In chain ( $R_{\perp}$ ) was from  $I_{43}$  and  $V_{12}$ ,  $R_{\perp} = dV_{12}/dI_{43}$ . Open squares in the  $I$ - $V$  curves stand for  $R_{\parallel}$  and filled circles are for  $R_{\perp}$ .

The anisotropy of resistance was clearly observed at any temperatures, while the ratio  $R_{\perp}/R_{\parallel}$  changes with temperature. The measured resistance is a sum of those of Si substrate, the surface space-charge layer, and the surface states.<sup>3</sup> Since, however, the conductivities of the substrate and the space-charge layer are isotropic, the anisotropy comes from the surface state. The  $R_{\parallel}$  increases with cooling while  $R_{\perp}$  show a minimum around 120 K. Thus the temperature dependences of conduction along and across the In chains are different, meaning different mechanisms of electrical conduction. The details of the data and analysis will be reported elsewhere.<sup>26</sup>

#### IV. SUMMARY

We have newly developed an independently driven four-tip STM system featuring liquid He cooling system, which cools the sample and tips down to 7 K. An integrated controller for the multitip STM combined with SEM has also been developed, which allows the tips to work as both STM

tips and electric probes for conductivity measurements. As a demonstration, atomic-resolution STM images were obtained with simultaneous operation. The temperature dependences of electrical conduction in different directions of an anisotropic surface have been measured by the square-4PP method. The abilities to measure conductivity at various temperatures with various arrangements of four tips are useful for analyzing electrical properties of various kinds of nanostructures and nanodevices as well as surfaces.

#### ACKNOWLEDGMENTS

This work was supported in part by the SENTAN Program of the Japan Science and Technology Agency and Grants-in-Aid for Scientific Research from the Japanese Society for the Promotion of Science.

- <sup>1</sup>A. V. Ermakov and B. J. Hinch, *Rev. Sci. Instrum.* **68**, 1571 (1997).
- <sup>2</sup>R. J. Collier and D. G. Hasko, *J. Appl. Phys.* **91**, 2547 (2002).
- <sup>3</sup>S. Hasegawa and F. Grey, *Surf. Sci.* **500**, 84 (2002).
- <sup>4</sup>Y. Ju, K. Inoue, M. Saka, and H. Abé, *Appl. Phys. Lett.* **81**, 3585 (2002).
- <sup>5</sup>T. Tanikawa, I. Matsuda, R. Hobara, and S. Hasegawa, *e-J. Surf. Sci. Nanotechnol.* **1**, 50 (2003).
- <sup>6</sup>A. Bachtold, M. S. Fuhrer, S. Plyasunov, M. Forero, E. H. Anderson, A. Zettl, and P. L. McEuen, *Phys. Rev. Lett.* **84**, 6082 (2000).
- <sup>7</sup>X. Lin *et al.*, *Appl. Phys. Lett.* **89**, 043103 (2006).
- <sup>8</sup>O. Guise, H. Marbach, J. T. Yates Jr., M.-C. Jung, J. Levy, and J. Ahner, *Rev. Sci. Instrum.* **76**, 045107 (2005).
- <sup>9</sup>M. Ishikawa, M. Yoshimura, and K. Ueda, *Jpn. J. Appl. Phys., Part 1* **44**, 1502 (2005).
- <sup>10</sup>K. Takami, M. Akai-Kasaya, A. Saito, M. Aono, and Y. Kuwahara, *Jpn. J. Appl. Phys., Part 2* **44**, L120 (2005).
- <sup>11</sup>O. Kubo, Y. Shingaya, M. Nakaya, M. Aono, and T. Nakayama, *Appl. Phys. Lett.* **88**, 254101 (2006).
- <sup>12</sup>I. Shiraki, F. Tanabe, R. Hobara, T. Nagao, and S. Hasegawa, *Surf. Sci.* **493**, 633 (2001).
- <sup>13</sup>H. Grube, B. C. Harrison, J. Jia, and J. J. Boland, *Rev. Sci. Instrum.* **72**, 4388 (2001).
- <sup>14</sup>S. Hasegawa, I. Shiraki, F. Tanabe, and R. Hobara, *Curr. Appl. Phys.* **2**, 465 (2002).
- <sup>15</sup>T. Kanagawa, R. Hobara, I. Matsuda, T. Tanikawa, A. Natori, and S. Hasegawa, *Phys. Rev. Lett.* **91**, 036805 (2003).
- <sup>16</sup>I. Matsuda, M. Ueno, T. Hirahara, R. Hobara, H. Morikawa, C. Liu, and S. Hasegawa, *Phys. Rev. Lett.* **93**, 236801 (2004).
- <sup>17</sup>R. Hobara, S. Yoshimoto, S. Hasegawa, and K. Sakamoto, *e-J. Surf. Sci. Nanotechnol.* **5**, 94 (2007).
- <sup>18</sup>T. Ikuno *et al.*, *Jpn. J. Appl. Phys., Part 2* **43**, L644 (2004).
- <sup>19</sup>Y. Murata *et al.*, *Jpn. J. Appl. Phys., Part 1* **44**, 5336 (2005).
- <sup>20</sup>S. Yoshimoto *et al.*, *Jpn. J. Appl. Phys., Part 2* **44**, L1563 (2005).
- <sup>21</sup>S. Yoshimoto *et al.*, *Nano Lett.* **7**, 956 (2007).
- <sup>22</sup>M. Carlà, L. Lanzi, E. Pallecchi, and G. Aloisi, *Rev. Sci. Instrum.* **75**, 497 (2004).
- <sup>23</sup>D.-J. Kim and J.-Y. Koo, *Rev. Sci. Instrum.* **76**, 023703 (2005).
- <sup>24</sup>H. W. Yeom *et al.*, *Phys. Rev. Lett.* **82**, 4898 (1999).
- <sup>25</sup>T. Tanikawa, I. Matsuda, T. Kanagawa, and S. Hasegawa, *Phys. Rev. Lett.* **93**, 016801 (2004).
- <sup>26</sup>R. Hobara, N. Nagamura, I. Matsuda, and S. Hasegawa, (to be submitted).